Optimization of concurrently compressed and torqued rod

Vladimir Kobelev (kobelev@imr.mb.uni-siegen.de)
University of Siegen https://orcid.org/0000-0002-2653-6853

Research Article

Keywords: structural optimization, optimization of compressed and twisted rods, eigenvalue optimization

Posted Date: November 24th, 2021

DOI: https://doi.org/10.21203/rs.3.rs-1106993/v1

Version of Record: A version of this preprint was published at Multidiscipline Modeling in Materials and Structures on February 7th, 2022. See the published version at https://doi.org/10.1108/MMMS-12-2021-0205.

Optimization of concurrently compressed and torqued rod

V. Kobelev[1]

Abstract

The applications of this method for stability problems in the context of twisted and compressed rods are demonstrated in this manuscript. The complement for Euler's buckling problem is Greenhill's problem, which studies the forming of a loop in an elastic bar under simultaneous torsion and compression (Greenhill, 1883). We search the optimal distribution of bending flexure along the axis of the rod. For the solution of the actual problem the stability equations take into account all possible convex, simply connected shapes of the cross-section. We study the cross-sections with equal principle moments of inertia. The cross-sections are similar geometric figures related by a homothetic transformation with respect to a homothetic center on the axis of the rod and vary along its axis. The cross section that delivers the maximum or the minimum for the critical eigenvalue must be determined among all convex, simply connected domains. The optimal form of the cross-section is known to be an equilateral triangle. The distribution of material along the length of a twisted and compressed rod is optimized so that the rod must support the maximal moment without spatial buckling, presuming its volume V remains constant among all admissible rods. The static Euler's approach is applicable for simply supported rod (hinged), twisted by the conservative moment and axial compressing force. For determining the optimal solution, we directly compare the twisted rods with the different lengths and cross-sections using the invariant factors. The solution of optimization problem for simultaneously twisted and compressed rod is stated in closed form in terms of the higher transcendental functions.

1. Twisted and axially compressed rod with an arbitrary convex simply-connected cross-section

Consider a thin elastic rod with isotropic cross-section, twisted by couples applied at its ends alone (Greenhill's problem. The problems of optimizing stability of the simply supported twisted rod were studied numerically in (Banichuk, Barsuk, 1982a). The rod possessed the similarly shaped cross-sections with the varying cross-sectional area. More advanced problem of twisted and compressed rod was studied numerically in (Banichuk, Barsuk, 1982b). The optimization problem consisted in finding the distribution of cross-sectional areas that assigns the largest value to the critical moment causing a loss of stability and such that the constraint on the volume of material and the constraints on the admissible thickness of the rod were satisfied.

The problem of determining the simultaneously compressed and twisted column of maximal efficiency was studied in (Spasic, 1993). Following the structural optimization theory, the shape of the column of minimal was determined numerically for a given combination of compression and torque.

The problem of the optimal design of columns under combined compression and torsion was investigated in (Kruzelecki, Ortwein, 2012). A cross-sectional area varying along the axis of the column which leads to the maximal critical loading was sought. The varying cross-section was approximated by a function with free parameters. Alternatively, the varying cross-section was determined numerically using Pontriagin's maximum principle.

Consider a thin elastic rod with isotropic cross-section, twisted by couples and compressed by axial forces applied at its ends (Greenhill's problem) (Pastrone, 1992). The twisting couple M and axial force Λ retain their initial direction during buckling and the boundary conditions of fixed axes of rotation are satisfied (Ziegler, 1977, Cases 1 and 2 in Table 1.1, Section 1.2, page 5). According to Euler's theory, the magnitude of the critical moment is determined by the smallest positive eigenvalue Λ. We search the closed-form analytical solutions for the optimal shape of the rod along its axis with the application of

[1] University of Siegen, Germany, Vladimir.kobelev@uni-siegen.de

the variational methods.). According to Euler's theory, the magnitude of the critical moment is determined by the smallest positive eigenvalue Λ. We demonstrate at the beginning the validity of static Euler's approach for simply supported rod (hinged), twisted by the conservative moment. The distribution of material along the length of a twisted rod is optimized so that the rod is of the constant volume V and will support the maximal moment without spatial buckling. The cross section that delivers the maximum or the minimum for the critical eigenvalue must be determined among all convex, simply connected domains. A priori form of the cross-section remains unknown. For the solution of the actual problem the stability equations take into account all possible convex, simply connected shapes of the cross-section. Thus, we drop the assumption about the equality of principle moments of inertia for the cross-section. The cross-sections are similar geometric figures related by a homothetic transformation with respect to a homothetic center on the axis of the rod and vary along its axis. The area of some reference cross-section Ω is A_0. The area $\mathcal{A}$ of the cross-section with the coordinate x is

$$\mathcal{A} = a(x)\mathcal{A}_0, 0 < a < 1 - L \le x \le L.$$

The dimensionless trial function $a(x)$ is positive, locally integrable function. Its integral over the half-length of the rod reads:

$$\mathcal{V}[a] = \int_0^L a(x)dx. \qquad (1)$$

We assume for briefness, that principal moments of inertia of the all cross-sections are equal:

$$J_1 = J_2 = j,\ j = \varkappa_\alpha a^\alpha.$$

The above equality is valid for the cross-sections in form of equilateral triangles and circles. The optimal shape of cross-section is the equilateral triangle as stated by (Ting,1963)

Consider the beam hinged on two supports $x = L$ and $x = -L$ (**Figure 1**):

$$\begin{aligned} &y|_{x=L} = 0, && y|_{x=-L} = 0,\\ &Ejy''|_{x=L} = 0, && Ejy''|_{x=-L} = 0,\\ &z|_{x=L} = 0, && z|_{x=-L} = 0,\\ &Ejz''|_{x=L} = 0, && Ejz''|_{x=-L} = 0. \end{aligned} \qquad (2)$$

The buckling equations the beam read

$$(Ejy'')'' = \widetilde{\mathrm{M}}z''' + \Lambda y'', \qquad (Ejz'')'' = -\widetilde{\mathrm{M}}y''' + \Lambda z'''. \qquad (3)$$

For the boundary value problem (7), (8), the actual curvatures and displacements y^*, z^* minimize the quotient:

$$\Lambda[j,\tilde{y},\tilde{z}] = \frac{\int_{-L}^{L}\left[Ej\left(\tilde{y}''^2 + \tilde{z}''^2\right) + 2\mathrm{M}(\tilde{z}'\tilde{y}'' - \tilde{z}''\tilde{y}')\right]dx}{\int_{-L}^{L}\left(\tilde{y}'^2 + \tilde{z}'^2\right)dx}, \qquad (4)$$

$$\Lambda[j,\mathrm{Y},Z] \equiv \Lambda[k_\alpha a^\alpha, y, z] = \min_{\tilde{y},\tilde{z}} \Lambda[j,\tilde{y},\tilde{z}].$$

The Euler's static approach is proved to be valid for the considered boundary value problem with conditions of fixed axes of rotation, Cases 1 and 2 (Ziegler, 1977, §5.4, Table 5.1, Section 1.2, page 127). The corresponding boundary-value problems are neither selfadjoint nor conservative in the classical sense. This load are referred to as the conservative system of the second kind (Leipholz, 1974).

2. Optimization problem and isoperimetric inequality for stability

Based on the above solution, the distribution of material along the length of a twisted rod will be optimized. We search the rod is of constant volume $2\mathcal{A}_0\mathcal{V}$ that support the maximal axial force Λ without spatial buckling, assuming the torsion moment M is given. The mass $\mathcal{M}$ of the rod is given by

$$\mathcal{M} = 2\rho\mathcal{A}_0\mathcal{V} = \text{const}, \tag{5}$$

The formal formulation of the optimization problem is the following:

$$\Lambda[\varkappa_\alpha a^\alpha, y, z] \to \max_{a(t)}. \tag{6}$$

The distribution of material along the length of a twisted rod is optimized so that the rod is of constant volume and provides the maximal moment without spatial buckling. Due to the mirror symmetry of the problem with respect to the point $x = 0$, one half of the rod $0 \le x \le L$ could be studied. The half-volume of the rod is $\mathcal{V}$. The augmented functional for the optimization problem (5)-(6) reads:

$$\mathcal{L}[A] = \mathcal{V}[a] + \lambda\Lambda[\varkappa_\alpha a^\alpha, y, z] = \int_0^L a(x)\, dx + \lambda \frac{\int_0^L \left[Ej\left(\tilde{y}''^2 + \tilde{z}''^2\right) + 2\mathrm{M}\left(\tilde{z}'\tilde{y}'' - \tilde{z}''\tilde{y}'\right)\right] dx}{\int_{-L}^L \left(\tilde{y}'^2 + \tilde{z}'^2\right) dx}. \tag{7}$$

The first variation of the augmented Lagrangian (7) reads:

$$\delta\mathcal{L}[A] = \int_0^L \delta a(x)\, dx + \lambda \frac{\int_0^L \delta(Ej)\cdot\left(\tilde{y}''^2 + \tilde{z}''^2\right) dx}{\int_0^L \left(\tilde{y}'^2 + \tilde{z}'^2\right) dx},$$

$$\delta(Ej) = E\varkappa_\alpha \delta(a^\alpha) = aE\varkappa_\alpha a^{\alpha-1}\delta a.$$

Let optimal distribution of the cross-sectional area along the span of the rod is $\mathrm{A}(x)$ .The necessary optimality condition follows from the vanishing of the first variation:

$$-c + A^{\alpha-1}\mathrm{K}^2 = 0, \tag{8}$$

with an auxiliary constant:

$$\mathrm{c} = (E\varkappa_\alpha \alpha)^{-1}\lambda.$$

The spatial curvature in Eq. (8) reads:

$$\mathrm{K}^2 = \kappa_y{}^2 + \kappa_z{}^2 = \tilde{y}''^2 + \tilde{z}''^2.$$

The application of the Fermat's principle for the optimization problems leads to the necessary optimality condition:

$$A = (\mathrm{K}/c)^{2/(1-\alpha)} \; . \tag{9}$$

The necessary optimality condition (9) is the requirement that the augmented Lagrangian has a stationary value. The optimal second moment of the cross-section follows from Eq. (9) as:

$$J = E\varkappa_\alpha \cdot (\mathrm{K}/c)^{2\alpha/(1-\alpha)} = \left(y''^2 + z''^2\right)^{\alpha/(1-\alpha)}. \tag{10}$$

The applied method of scaling allows an arbitrary selection of the constant c. For briefness of the governing equations, we set the constant c as the positive solution of the equation:

$$E\alpha\varkappa_\alpha (1/c)^{2\alpha/(1-\alpha)} = 1.$$

With this choice the bending stiffness reduces to:

$$J = \left(y''^2 + z''^2\right)^{\alpha/(1-\alpha)} \equiv \mathrm{K}^{2\alpha/(1-\alpha)}. \tag{11}$$

3. Closed-form solution of the governing equations

The order of both equations (8) could be reduced by one using the boundary value conditions (7). The buckling equations transform with Eq. (16) to:

$$e_1[z'', y''] = \left(y''^2 + z''^2\right)^{\alpha/(1-\alpha)} y'' - \Lambda y'' + \mathrm{M}z''', \tag{12}$$

$$e_2[z'', y''] = \left(y''^2 + z''^2\right)^{\alpha/(1-\alpha)} z'' - \Lambda z'' - \mathrm{M}y'''. \tag{13}$$

For the handling of the governing equations, we introduce the new dimensionless parameter Ω:

$$\Omega = \frac{\Lambda}{3}\left(\frac{2}{\mathrm{M}}\right)^2. \tag{14}$$

If solely a axial force compresses the rod, the Euler's eigenvalue Λ determines the buckling compression. Otherwise, if only a moment twists the rod, the buckling state results from the eigenvalue of the pure Greenhill problem M. If both loads are simultaneously applied, the parameter Ω relates two critical buckling states. The eigenvalue of the pure Greenhill problem M follows from the Euler's eigenvalue Λ with this parameter Ω:

$$\mathrm{M} = 2\sqrt{\frac{\Lambda}{3\Omega}}.$$

The analysis of the solution simplifies with the parameter Ω. Two mentioned above pure solutions result as the opposite limit cases from the general formulas. One asymptotic case will be $\Omega \to \infty$, $\Lambda \to \infty$. If the torsional eigenvalue M remains bonded, this case corresponds to the solution of the Greenhill problem of the pure twisted rod. The axial compression disappears in this case. The instability of rod appears due to action of the twisting moment.

The other asymptotic case is $\Omega \to 0$, $\mathrm{M} \to \infty$. If the compression eigenvalue Λ is bonded, this case corresponds to the solution of the Euler problem of the pure compressed rod. In this case the torque is absent and the instability is caused only by the axial compression.

Now we proceed with the solution of optimization problem. For the solution of two simultaneous equations (12),(13) we select two auxiliary functions $\mathrm{K}(x), \theta(x)$:

$$z'' = \mathrm{K}\cos\theta, y'' = \mathrm{K}\sin\theta. \tag{15}$$

After the substitution (15) into (12) and (13), we get the differential equations for the auxiliary functions $\mathrm{K}(x), \theta(x)$. It is possible to solve these equations for K, θ, but we prefer to find the solution for the functions A, θ. With this choice of the unknowns, the solution immediately results to the optimal cross-section area A . Using Eq. (9), we replace for this purpose K by A:

$$A\theta'' + (\alpha+1)\theta' A' + (\alpha-1)\sqrt{\frac{\Lambda}{3\Omega}} A' A^{-\alpha} \quad = 0, \tag{16}$$

$$A'' + \frac{\alpha-1}{2A} A'^2 - \frac{2A}{\alpha+1}\theta'^2 + \frac{4}{1+\alpha}\sqrt{\frac{\Lambda}{3\Omega}} A^{1-\alpha}\,\theta' + \frac{2\Lambda A^{1-\alpha}}{1+\alpha} = 0. \tag{17}$$

Eq. (16) leads to the solution for function θ. The integration constant could be put to zero from the symmetry considerations: $\theta(0) = 0$. We denote the solution of the equation (16) as $\vartheta(x)$. The solution reads:

$$\vartheta = (1-\alpha)\sqrt{\frac{\Lambda}{3\Omega}} \int_0^x A^{-\alpha}(z)\, dz. \tag{18}$$

Substitution of the solution $\vartheta(x)$ from Eq. (18) into the Eq. (17) leads to the nonlinear ordinary differential equation only for the function A:

$$A'' + \frac{\alpha-1}{2A} A'^2 - 2A + \frac{2A}{\alpha+1} A^{1-\alpha} - \frac{2\Lambda(1-\alpha)}{3\Omega} A^{1-2\alpha} = 0. \tag{19}$$

The Eq. (19) contains three dimensionless parameters: α, Ω, Λ. The critical value for M results with Eq. (14). For the closed form solution, the dependent and independent variables in Eq. (19) must be exchanged:

$$\frac{d^2x}{dA^2} = \frac{\alpha-1}{2A}\frac{dx}{dA} + 2\Lambda \frac{(1-\alpha^2)A^{1-2\alpha} + 3\Omega A^{1-\alpha}}{3\,\Omega\,(1+\alpha)} \left(\frac{dx}{dA}\right)^3. \tag{20}$$

Eq. (20) is of the second order with missing dependent and independent variables. The reduction of order leads to the nonlinear ordinary differential equation of the first order in terms of $\Xi = \frac{dx}{dA}$:

$$\frac{d\Xi}{dA} = \frac{\alpha-1}{2A}\Xi + 2\Lambda \frac{(1-\alpha^2)A^{1-2\alpha} + 3\Omega A^{1-\alpha}}{3\,\Omega\,(1+\alpha)} \Xi^3. \tag{21}$$

The dependent and independent variables Ξ, A in Eq. (21) are separable. The differential equation (21) is solvable by quadrature:

$$\int_{C_1}^{\Xi(A)} \frac{d\xi}{\frac{\alpha-1}{2A}\xi+2\Lambda\frac{(1-\alpha^2)A^{1-2\alpha}+3\Omega A^{1-\alpha}}{3\,\Omega\,(1+\alpha)}\xi^3} = A,$$

$$x = \int_0^A \Xi(a)\mathrm{da} + C_2 \ . \tag{22}$$

The integral (22) contains two integration constants: $C_1,\ C_2$. The integral for the Eq. (22) is summable, if the first integration constant is equal to:

$$C_1 = \frac{4\Lambda}{3\Omega}\frac{3\Omega+1+\alpha}{1+\alpha}. \tag{23}$$

With this value, the solution of the Eq. (20) reads:

$$x = \frac{1}{2\sqrt{\Lambda}}\int_0^A \frac{a^{\alpha-1}}{\sqrt{a^{\alpha-1}(1+\alpha+3\Omega)-3a^{\alpha}\,\Omega-1-\alpha}}da + C_2 \quad \text{for } 0 < A < 1, \text{ right half} \tag{24}$$

$$x = -\frac{1}{2\sqrt{\Lambda}}\int_0^A \frac{a^{\alpha-1}}{\sqrt{a^{\alpha-1}(1+\alpha+3\Omega)-3a^{\alpha}\,\Omega-1-\alpha}}da + C_2 \text{ for } 0 < A < 1, \text{ left half} \tag{25}$$

The function $A(x)$, which is defined implicitly with Eq. (24), (25), is an even function of x according the symmetry conditions. Consequently, according to the symmetry of the solution, dA/dx must vanish in the point $x = 0$. The resulting equation of the first order is solvable in quadrature:

$$x = \frac{1}{2\sqrt{\Lambda}}\int_0^A \frac{a^{\alpha-1}}{\sqrt{a^{\alpha-1}(1+\alpha+3\Omega)-3a^{\alpha}\,\Omega-1-\alpha}}da \quad \text{for } 0 < A < 1, \text{ right half} \tag{26}$$

$$x = -\frac{1}{2\sqrt{\Lambda}}\int_0^A \frac{a^{\alpha-1}}{\sqrt{a^{\alpha-1}(1+\alpha+3\Omega)-3a^{\alpha}\,\Omega-1-\alpha}}da \quad \text{for } 0 < A < 1, \text{ left half} \tag{27}$$

The functions in Eqs. (26)..(27) are the real functions of $0 < A < 1$. The limit in Eq. (28) is the right-hand limit $\alpha \to 1+$. The area of the optimal cross-sections vanishes in the end points of the rod, where the bending moment disappears:

$$x(A = 0) = L\ . \tag{28}$$

The formulas (26) and (27) provide the most general expression for the solution of the declared optimization problem for all admissible values of parameters α, Λ, Ω. For an arbitrary value of parameter α, the expression in terms of the standard transcendental functions seems to be impossible. In the following, we find the closed form solutions with higher transcendental functions in the cases, significant for application.

4. Special cases

4.1. Greenhill stability special case

At first, the mentioned above Euler and pure Greenhill load buckling states result from the general expressions (26) and (27) as the special cases.

The solution (26) reduces in the asymptotic case $\Omega \to \infty$ to the solution of the optimization problem for the pure twisted rod with the vanishing axial compression. The singular integral in (26) and (27) expresses in terms of the higher functions (Gradstein, Ryzhik, 2014):

$$x = \frac{1}{2\sqrt{3\Omega\Lambda}} \int_0^A \frac{a^{\alpha-1}}{\sqrt{a^{\alpha-1}-a^{\alpha}}} da = \frac{\sqrt{3}}{6\sqrt{\Omega\Lambda}} \int_0^A \frac{a^{\frac{\alpha-1}{2}}}{\sqrt{1-a}} da \quad \text{for } 0 < A < 1, \text{ right half,}$$

$$x = \frac{2\sqrt{A^{\alpha+1}}}{3\mathrm{M}\Omega(\alpha+1)}\, {}_2F_2\left(\left[\frac{1}{2}, \frac{\alpha+1}{2}\right], \left[\frac{3+\alpha}{2}\right], A\right), \quad for \quad \alpha > 1,$$

$$L = \frac{\sqrt{3}}{6\sqrt{\Omega\Lambda}} \int_0^1 \frac{a^{\frac{\alpha-1}{2}}}{\sqrt{1-a}} da = \frac{2}{3\mathrm{M}\Omega} \mathrm{B}\left(\frac{1}{2}, \frac{\alpha+1}{2}\right), \tag{29}$$

$$X = \frac{x}{L} = \frac{2\sqrt{A^{\alpha+1}}}{\alpha+1} \frac{{}_2F_2\left(\left[\frac{1}{2}, \frac{\alpha+1}{2}\right], \left[\frac{3+\alpha}{2}\right], A\right)}{\mathrm{B}\left(\frac{1}{2}, \frac{\alpha+1}{2}\right)}.$$

The solution (29) is the solution of the optimization problem for the twisted rod with the vanishing axial compression.

4.2. Euler stability special case

Similarly, the other asymptotic case $\Omega \to 0$ delivers the solution of the optimization problem for the solely compressed rod with the zero torque. The singular integral in Eqs. (26)-(27) could be expressed to the higher functions:

$$x = \frac{1}{2\sqrt{(1+\alpha)\Lambda}} \int_0^A \frac{a^{\alpha-1}}{\sqrt{a^{\alpha-1}-1}} da \quad \text{for } 0 < A \le 1, \text{ right half} \tag{30}$$

The integral in Eq. (30) can be found with the hypergeometric function (Gradstein, Ryzhik, 2014):

$$x = \frac{iA^{\alpha}}{2\alpha\sqrt{(1+\alpha)\Lambda}}\, {}_2F_2\left(\left[\frac{1}{2}, \frac{\alpha}{\alpha-1}\right], \left[\frac{2\alpha-1}{\alpha-1}\right], A^{\alpha-1}\right), \qquad \alpha > 1. \tag{31}$$

The half-length of the rod follows from (31) as the limit value $A = 1$:

$$L = \frac{1}{2\sqrt{(1+\alpha)\Lambda}} \int_0^1 \frac{a^{\alpha-1}}{\sqrt{a^{\alpha-1}-1}} da = \frac{i}{2\sqrt{(1+\alpha)\Lambda}\,(1-\alpha)} \mathrm{B}\left(\frac{1}{2}, \frac{\alpha}{\alpha-1}\right). \tag{32}$$

From Eqs. (31) and (32) follows the normalized coordinate ($0 \le X \le 1$):

$$X = \frac{x}{L} = \frac{1-\alpha}{\alpha} \frac{A^{\alpha}}{\mathrm{B}\left(\frac{1}{2}, \frac{\alpha}{\alpha-1}\right)}\, {}_2F_2\left(\left[\frac{1}{2}, \frac{\alpha}{\alpha-1}\right], \left[\frac{2\alpha-1}{\alpha-1}\right], A^{\alpha-1}\right). \tag{33}$$

5. General cases an arbitrary Ω

5.1. General solution for case $\alpha = 1$

The closed form solution of the principal Eqs. (26)..(27) could be obtained for the practically interesting cases $\alpha = 1,2,3$.

In the case $\alpha = 1$ the solution reads (**Figure 2**):

$$x = \frac{1}{2\sqrt{3\Omega\Lambda}} \int_0^A \frac{1}{\sqrt{1-a}} da = \frac{1}{\sqrt{3\Omega\Lambda}} \left(1 - \sqrt{1-A}\right) \text{ for } 0 < A < 1, \text{ right half.} \tag{34}$$

The half-length of the rod follows from (34) as:

$$L = \frac{1}{2\sqrt{3\Omega\Lambda}} \int_0^1 \frac{1}{\sqrt{1-a}} da = \frac{1}{\sqrt{3\Omega\Lambda}}, \tag{35}$$

The relation of the normalized coordinate to the optimal cross-section is a quadratic function:

$$X \equiv \frac{x}{L} = 1 - \sqrt{1-A}, A = 2X - X^2, \tag{36}$$

The half-volume of the optimal rod evaluates trivially to:

$$\mathcal{V}_{\alpha=1} = \frac{1}{2\sqrt{3\Omega\Lambda}} \int_0^A \frac{a}{\sqrt{1-a}} da = \frac{2\sqrt{3}}{9\sqrt{\Omega\Lambda}},$$

$$\mathcal{v}_{\alpha=1} = \frac{\mathcal{V}_{\alpha=1}}{L} = \int_0^1 A dX = \frac{2}{3}. \tag{37}$$

Notably, that the shape in the case $\alpha = 1$ does not depend on the parameter Ω.

5.2. General solution for case $\alpha = 2$

In the case $\alpha = 2$, the solution reads (**Figure 3**):

$$x = \frac{\sqrt{3}}{6\sqrt{\Lambda}} \int_0^A \frac{1}{\sqrt{(1-a)(\Omega a - 1)}} da = -\frac{i\sqrt{3}}{12} \frac{\Upsilon(A,\Omega) - \Upsilon(0,\Omega)}{\sqrt{\Omega^3 \Lambda}}, \text{ for } 0 < A < 1, \text{ right half,}$$

$$L = -\frac{i\sqrt{3}}{12} \frac{\Upsilon(1,\Omega) - \Upsilon(0,\Omega)}{\sqrt{\Omega^3 \Lambda}}. \tag{38}$$

where the auxiliary function is:

$$\Upsilon(A,\Omega) = 2\sqrt{\Omega}\left(\sqrt{1-A}\sqrt{1-\Omega A}\right) - (1+\Omega) ln\left(1 + \Omega - 2A\Omega + 2\sqrt{\Omega}\sqrt{1-A}\sqrt{1-\Omega A}\right) \tag{39}$$

The shape of the optimal rod depends on the parameter Ω. If the Ω parameter is less than the critical value, $\Omega_2 = 1$, the functions of the cross-sectional area are roughly parabolic. Otherwise, the functions possess the saddle points. The shapes for the values of the parameter, less than critical $\Omega < \Omega_2 = 1$, are shown on upper half of **Figure 4** . If parameter is higher than critical value $\Omega > \Omega_2 = 1$, the shapes are plotted on the lower half of this figure. For comparison, both cases are shown overlapped on **Figure 5.**

With the Eqs. (38)..(39), the normalized axial coordinate $0 < X < 1$ of the cross-section A reads:

$$X(A,\Omega) \equiv \frac{x}{L} = \frac{\Upsilon(A,\Omega) - \Upsilon(0,\Omega)}{\Upsilon(1,\Omega) - \Upsilon(0,\Omega)}. \tag{40}$$

The volume of the rod is easily calculated with the integration of Eq. (3) by parts. Remembering that $A(0) = 1, X(0,\Omega) = 1$ we get the expression for the half-volume of the rod $\mathcal{V}_{\alpha=2}$. Dividing the half-volume of the rod by half-length, the normalized half-volume results:

$$\mathcal{v}_{\alpha=2} = \frac{\mathcal{V}_{\alpha=2}}{L} = 1 - \int_0^1 X(A,\Omega)dA\,. \tag{41}$$

The integral (42) allows the expression in closed form:

$$\mathcal{v}_{\alpha=2} = \frac{\left[4\sqrt{\Omega}(\Omega+1)(3\Omega^2+2\Omega+3)\chi_2 - 4\Omega(3\Omega^2+4\Omega+3)\right]\chi_1 + \left[8\Omega(3\Omega^2+4\Omega+3)\chi_2 - 12\Omega^{3/2}(\Omega+1)\right]}{\left[16\Omega^{3/2}(\Omega+1)^2\chi_2 - 16\Omega^2(\Omega+1)\right]\chi_1 + \left[32\Omega^2\chi_2 - 16\Omega^{5/2}\right]},$$

$$\chi_1 = \ln\left(1+\Omega-2\sqrt{\Omega}\right) + \ln(1-\Omega), \tag{42}$$

$$\chi_2 = \ln(1-\Omega).$$

The asymptotic case $\Omega \to 0$ delivers the solution of the optimization problem for the solely compressed rod with the zero torque. This solution is the limit case of (42) as $\Omega \to 0$:

$$\tilde{X} = \lim_{\Omega\to 0} X = 1 - \sqrt{1-A} - \frac{A}{2}\sqrt{1-A},$$

$$\widetilde{A} = A \underset{\Omega\to 0}{\approx} 1 - \left(\tilde{\sigma} + \frac{1}{\tilde{\sigma}}\right),\ \tilde{\sigma} = \sqrt[3]{\tilde{X} - 1 + \sqrt{\tilde{X}^2 - 2\tilde{X}}}, \tag{43}$$

$$\tilde{\mathcal{v}}_{\alpha=2} = \int_0^1 \widetilde{A}\,dX = \frac{4}{5}.$$

5.3. General solution for case $\alpha = 3$

Finally, we study the last practically interesting case $\alpha = 3$. For this case, the optimal shape is solvable in closed form. The governing equations (26)-(27) reduce in this case to the following integrals:

$$x = \frac{\sqrt{3}}{6\sqrt{\Lambda}}\int_0^A \frac{a^2}{\sqrt{(1-a)\left(\Omega a^2 - \frac{\Omega_3}{2}(a-1)\right)}}da \ \text{ for } 0 < A < 1, \text{ right half, with } \Omega_3 = \frac{8}{3}. \tag{44}$$

For the briefness of the formulas, we introduce the auxiliary variable $Z = \sqrt{3\Omega + 1}$. With the variable Z, the axial coordinate (44) rewrites as an integral with the variable upper limit:

$$x(A,\Omega) = \frac{1}{2\sqrt{\Lambda}}\int_0^A \frac{a^2}{\sqrt{(1-a)(aZ-a-2)(aZ+a+2)}}da \ \text{ for } 0 < A < 1, \text{ right half.} \tag{45}$$

Analogously, the half-length and the half-volume reduce to the similar integrals with the fixed limit of integration:

$$L(\Omega) = \frac{1}{2\sqrt{\Lambda}}\int_0^1 \frac{a^2}{\sqrt{(1-a)(aZ-a-2)(aZ+a+2)}}da \ \text{ for } 0 < A < 1, \text{ right half,} \tag{46}$$

$$\mathcal{v}_{\alpha=3}(\Omega) = \frac{1}{2\sqrt{\Lambda}}\int_0^1 \frac{a^3}{\sqrt{(1-a)(aZ-a-2)(aZ+a+2)}}da \text{ for } 0 < A < 1, \text{ right half.}$$

The integrals (45) and (46) express in closed form:

$$x(A,\Omega) = c_1 \cdot [\Phi(A) - \Phi(0)] + c_2.[\Psi(A) - \Psi(0)],$$

$$L(\Omega) = c_1 \cdot [\Phi(1) - \Phi(0)] + c_2.[\Psi(1) - \Psi(0)], \tag{47}$$

$$\mathcal{v}_{\alpha=3}(\Omega) = c_3 \cdot [\Phi(1) - \Phi(0)] + c_4[\Psi(1) - \Psi(0)], \tag{48}$$

The coefficients in Eq. (47)..(48) are :

$$c_1 = \frac{2}{3\sqrt{\Lambda}}\frac{(Z^2+3)\sqrt{Z+3}}{(1-Z)^{3/2}(Z+1)^2}, \qquad c_2 = \frac{2}{3\sqrt{\Lambda}}\frac{(Z^2+3)}{\sqrt{Z+3}(1-Z)^{3/2}(Z+1)},$$

$$c_3 = \frac{8}{15\sqrt{\Lambda}}\frac{(Z^2+3)^3\sqrt{Z+3}}{(1-Z)^{5/2}(Z+1)^3}, \qquad c_4 = \frac{8}{15\sqrt{\Lambda}}\frac{(Z^4+3Z^2+12)}{\sqrt{Z+3}(1-Z)^{5/2}(Z+1)^2} \tag{49}$$

The special functions $\Psi(A), \Phi(A)$ are the elliptic integrals of the first and second kinds correspondingly:

$$\Psi(A) = \mathbf{F}\left(\mathbb{Q}(A), \frac{1}{\mathbb{Q}(1)}\right), \qquad \Phi(A) = \mathbf{E}\left(\mathbb{Q}(A), \frac{1}{\mathbb{Q}(1)}\right),$$

$$\mathbb{Q}(A) = \frac{\sqrt{(Z-1)(2+(Z+1)A)}}{2\sqrt{Z}}. \tag{50}$$

The shape of the optimal rod depends on the parameter Ω. If the Ω parameter is less than the critical value $\Omega_3 = 8/3$, the functions of the cross-sectional area are roughly parabolic. Otherwise, the functions possess the saddle points. The shapes for the values of the parameter, less than critical $\Omega < \Omega_3$, are shown on upper half of **Figure 6** . If parameter is higher than critical value $\Omega > \Omega_3$, the shapes are plotted on the lower half of this figure. The combination of both cases is displayed on **Figure 7.**

6. Mass comparisons of optimal rods to the rods with the constant cross-sections

Evidently, that the exponent α influences the estimations for the optimization effects. For comparison, we need the expression of the volume of the loaded rods with different length. The rods possess the constant cross-section along their axes. The rods with the definite form of cross-section are compressed by the axial force F_C and twisted by moment M_T . The stability criterion for the simultaneously compressed and twisted rods reads (Grammel, 1923):

$$\left(\frac{M_T\ L}{Ej\ \pi}\right)^2 + \frac{2F_C L}{Ej\ \pi^2} \leq 1. \tag{51}$$

If the cross-sectional area if the constant rod is A_{ref}, the volume of the half of the rod will be $V_{ref} = A_{ref}L$. We substitute the values

$$Ej = \varkappa_\alpha A_{ref}^\alpha, \mathrm{M} \quad = \sqrt{\frac{4\Lambda}{3\Omega}}, , M_T = \varkappa_\alpha \mathrm{M},\ F_C = \varkappa_\alpha \Lambda$$

into Eq. (51) , After the substitution, we obtaining the expression of the stability criteria in terms of the compressional eigenvalue Λ and the dimensionless parameters which control the relation between the twist and compression load Ω:

$$\frac{4\Lambda\ \ L^2}{3\Omega A_{ref}^{2\alpha}\ \pi^2} + \frac{2\Lambda\ \ L}{A_{ref}^\alpha\ \pi^2} \leq 1. \tag{52}$$

Using the expressions (52) we get the critical compression load of the rod with the constant cross-section of the reference rod A_{ref}:

$$\Lambda_{ref} = \frac{3\Omega\pi^2 A_{ref}^{2\alpha}}{2A_{ref}\left(3A_{ref}^\alpha\Omega + 2L\right)}. \tag{53}$$

The cross-section of the uniform rod with the critical eigenvalue Λ_{ref} results from Eq. (53) after the solution this equation for A_{ref}. For comparison, we need the cross-section for the rods with $\Lambda_{ref} = 1$. The uniform cross-section of the rod with the half-length L and critical compression eigenvalue $\Lambda \quad = 1$ results from (53) as:

$$A_{ref} = \sqrt[\alpha]{L\frac{\sqrt{4\pi^2\Omega + 3\Omega^2} + 3\Omega}{3\pi^2\Omega}},$$

$$\mathcal{V}_{ref} = LA_{ref}, \mathcal{v}_{ref} = \frac{\mathcal{V}_{ref}}{L} = A_{ref}. \tag{54}$$

The half-volumes of the uniform rods $\mathcal{v}_{ref}$ with the half-length $L = 1$ and various values Ω and α are shown on **Figure 8**.

On the other hand, the volumes of the optimal rods $\mathcal{v}_\alpha(\Omega)$ for the same critical compression load $\Lambda = 1$ were already determined above and are given by Eqs. (37), (42) and (48). With this information we can relate the volumes of the rods with the optimal and with the uniform cross-sections. Subsequently, the masses of the twisted rods for the same half-length $L = 1$ and equal buckling forces are compared. The volumes and masses of the optimal and reference twisted rods relate to each other as:

$$\mathcal{R}(\alpha, \Omega) = \frac{\mathcal{v}_\alpha(\Omega)}{\mathcal{v}_{ref}}. \tag{55}$$

The masses of the optimal rods come from the Eqs. (38), (43) and (45). The values $\mathcal{R}$ are shown as the functions of α and Ω on **Figure 9**.

Alternatively, we can represent the values $\mathcal{R}$ as the functions of the ratios torque to compression loads $\frac{\mathrm{M}}{\sqrt{\Lambda}}$. For this purpose, the abscissa axis on **Figure 10** is scaled using the formula:

$$\frac{\mathrm{M}}{\sqrt{\Lambda}} \quad = \sqrt{\frac{4}{3\Omega}}.$$

Remarkably, that the optimal rods possess less mass, than the rods with the constant cross-sections only for definite values of the ratio Ω.

7. Conclusions

In this manuscript, the solution of optimization problem for twisted rod is stated in closed form. The solution expresses in terms of the higher transcendental functions. The final formulas involve the length of the rod, its volume and critical torque and axial compression force. Remarkable, that in the torsion stability problem the optimal shape of the rod is roughly parabolic along its length and the optimal shape of cross-section is the equilateral triangle.

7.1. References

Abramowitz, Milton; Stegun, Irene Ann, eds. (1983) Handbook of Mathematical Functions with Formulas, Graphs, and Mathematical Tables. Applied Mathematics Series. 55. Washington D.C.; New York: United States Department of Commerce, National Bureau of Standards; Dover Publications

Atanackovic T.M., Glavardanov V.B. (2002), Buckling of a twisted and compressed rod, International Journal of Solids and Structures 39 (2002) 2987–2999

Banichuk N., Barsuk A., Jeronen J., Tuovinen T., Neittaanmäki P. (2020) Stability of Axially Moving Materials, Some General Methods, Springer International Publishing, Cham

Banichuk N.V. (1990) Introduction to Optimization of Structures, New York: Springer-Verlag

Banichuk NV, Barsuk A.A. (1982a) On stability of torsioned elastic rods. In: Izvestiya Akademii Nauk SSSR, Mekhanika Tverdogo Tela (MTT) (6):148–154

Banichuk, N.V., Barsuk, A.A. (1982b) Optimization of stability of elastic beams against simultaneous compression and torsion. In: Applied Problems of Strength and Plasticity. Automation and algorithms for Solving Problems in Elastoplastic State (collection). Gorkii, Gorkii State University, 1982, pp. 122-126.

Beck M. (1955) Knickung Gerader Stäbe Durch Druck und Konservative Torsion. Ingenieur-Archiv, Band XXILI, Heft 4

Bullen P.S. (2003) Handbook of Means and Their Inequalities Mathematics and Its Applications. Dordrecht: Kluwer Academic Publishers

Coleman B.D., Dill E.H., Lembo M., Lu Z., Tobias I. (1993) On the Dynamics of Rods in the Theory of Kirchhoff and Clebsch, Arch. Rational Mech. Anal. 121 (1993)339-359

Glavardanov V.B, Maretic R. B., Grahovac N. M. (2009) Buckling of a twisted and compressed rod supported by Cardan joints, European Journal of Mechanics A/Solids 28 (2009) 131–140

Gradshtein I.S., Ryzhik I.M. (2014) Table of Integrals, Series, and Products. Academic Press, 2014, ISBN 0-12-384933-0

Grammel R. (1923) Das kritische Drillungsmoment von Wellen. Zeitschrift für angewandte Mathematik und Mechanik, Heft 4, Band 3

Greenhill A.G. (1883) On the strength of shafting when exposed both to torsion and to end thrust, Inst. Mech. Engineers, Proc., 182–225.

Kobelev V. (2012) Confirmation of Lagrange hypothesis for twisted elastic rod, Struct. Multidisc Optim, DOI 10.1007/s00158-012-0773-9

Kruzelecki J., Ortwein R. (2012) Optimal design of clamped columns for stability under combined axial compression and torsion, Struct. Multidisc. Optim. 45, 729–737

Pastrone F. (1992) Torsional instabilities of Greenhill type in elastic rods, Rendiconti del Seminario Matematico della Università di Padova, 87, p. 77-91

Spasic D.T. (1993) Stability of a compressed and twisted linearly-elastic rod, PhD thesis, University of Novi Sady

Ting T. W. (1963) Isoperimetric Inequality for Moments of Inertia of Plane Convex Sets, Transactions of the American Mathematical Society, Vol. 107, No. 3 (June 1963), pp. 421-431

Ziegler, H. (1977) Principles of structural stability. 2nd ed. Basel, Stuttgart: Birkhäuser, 1977

Figures

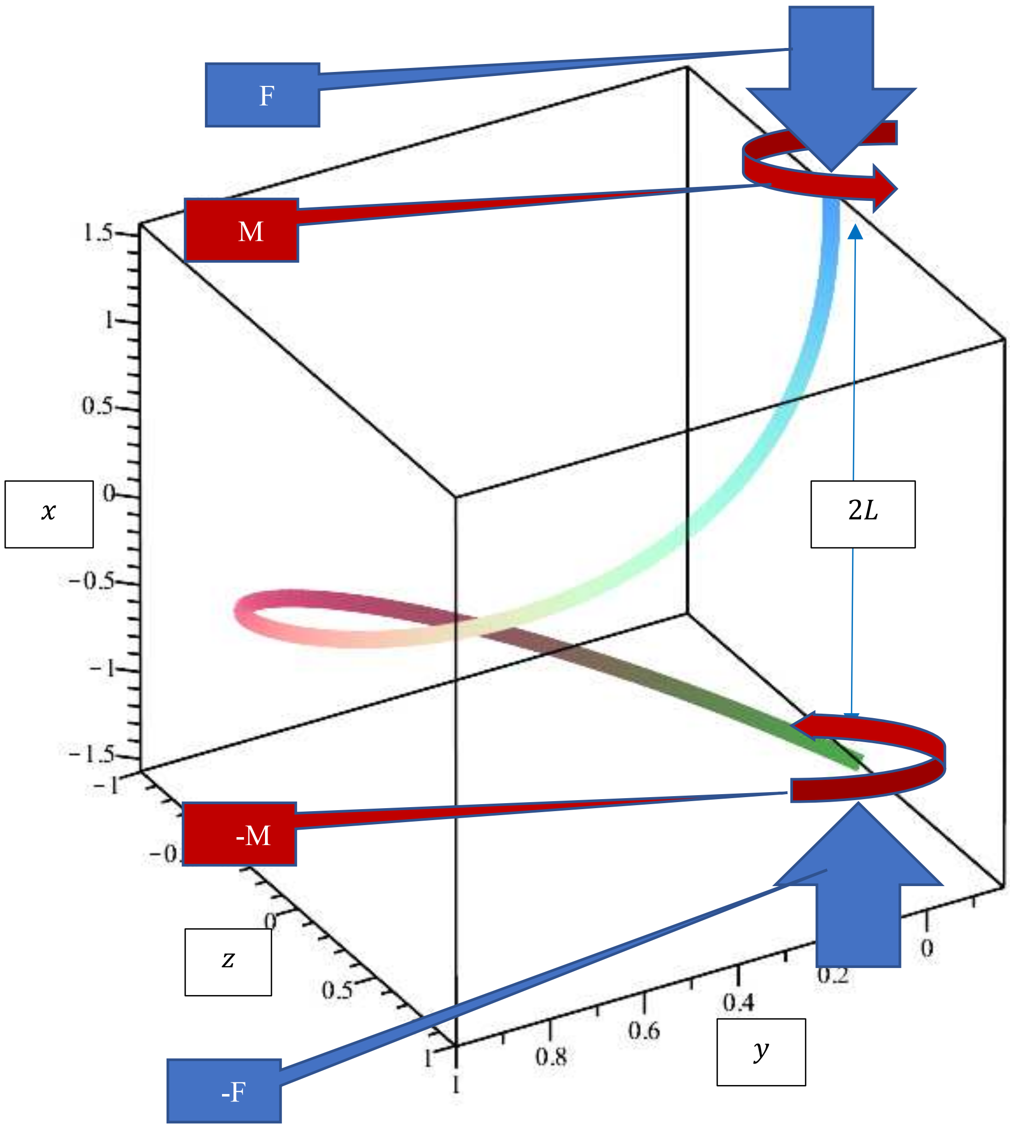

Figure 1 The buckling shape of the simultaneously twisted and compressed rod with the simply supported (hinged) ends

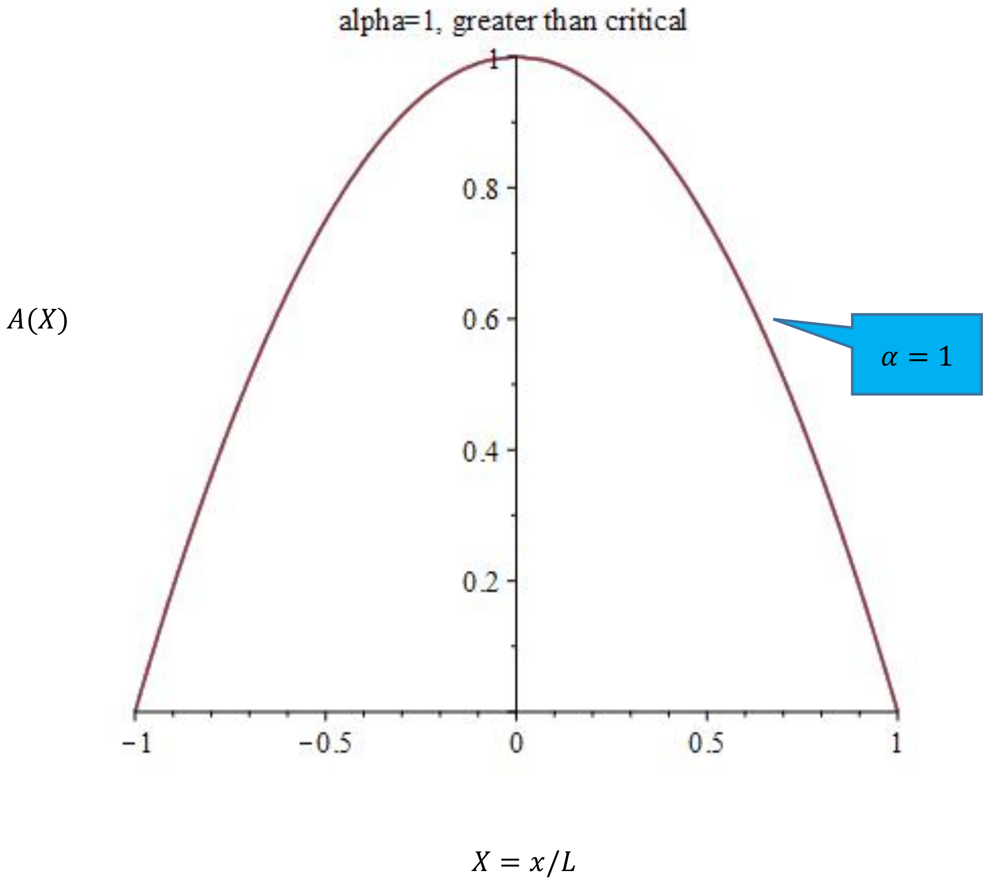

Figure 2 Areas of cross-sections of the optimal twisted rods for $\alpha = 1$ *for all values of parameter Ω*

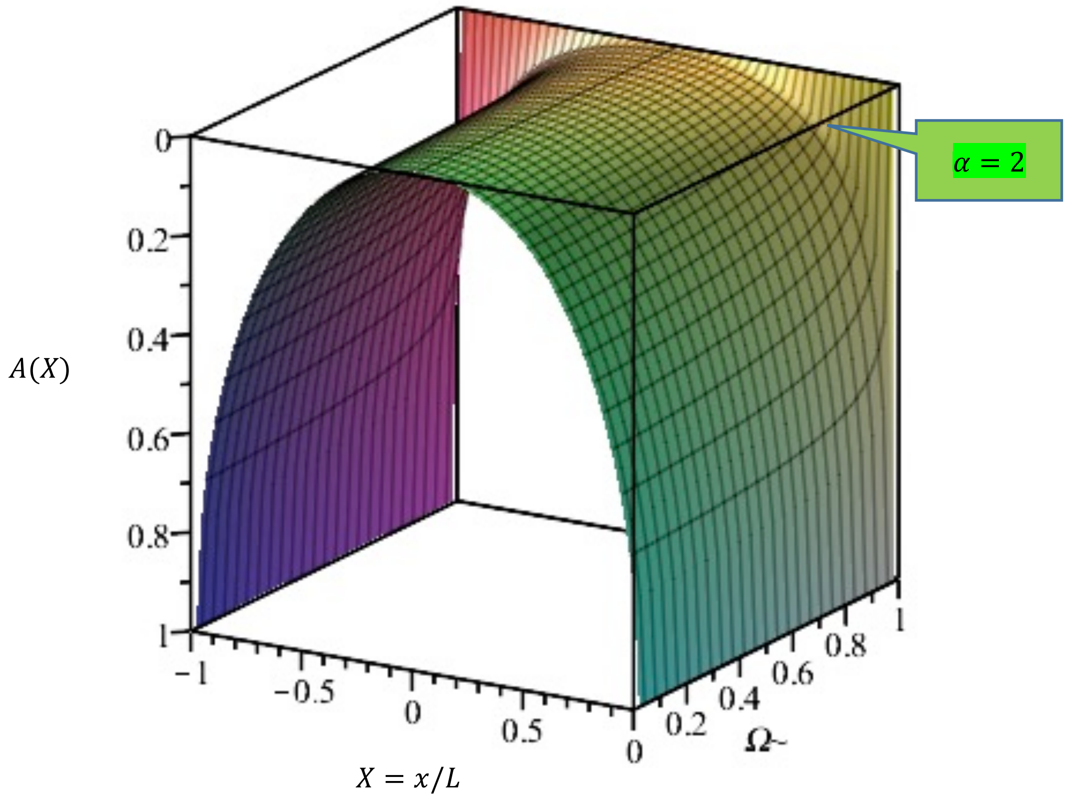

Figure 3 Areas of cross-sections of the optimal twisted rods for $\alpha = 2$ *for all values of parameter* Ω

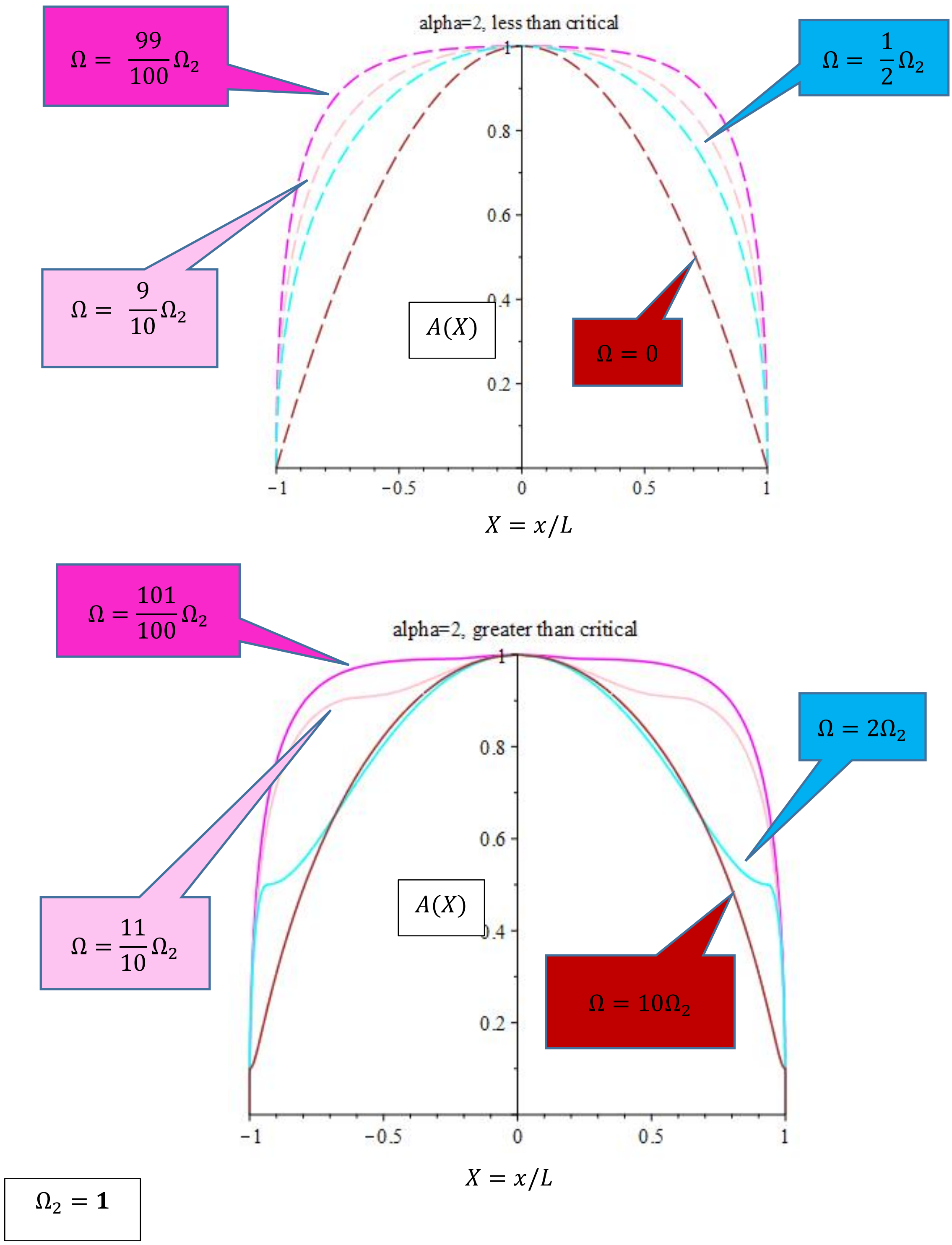

Figure 4 Areas of cross-sections of the optimal twisted rods for $\alpha = 2$ for all values of parameter Ω

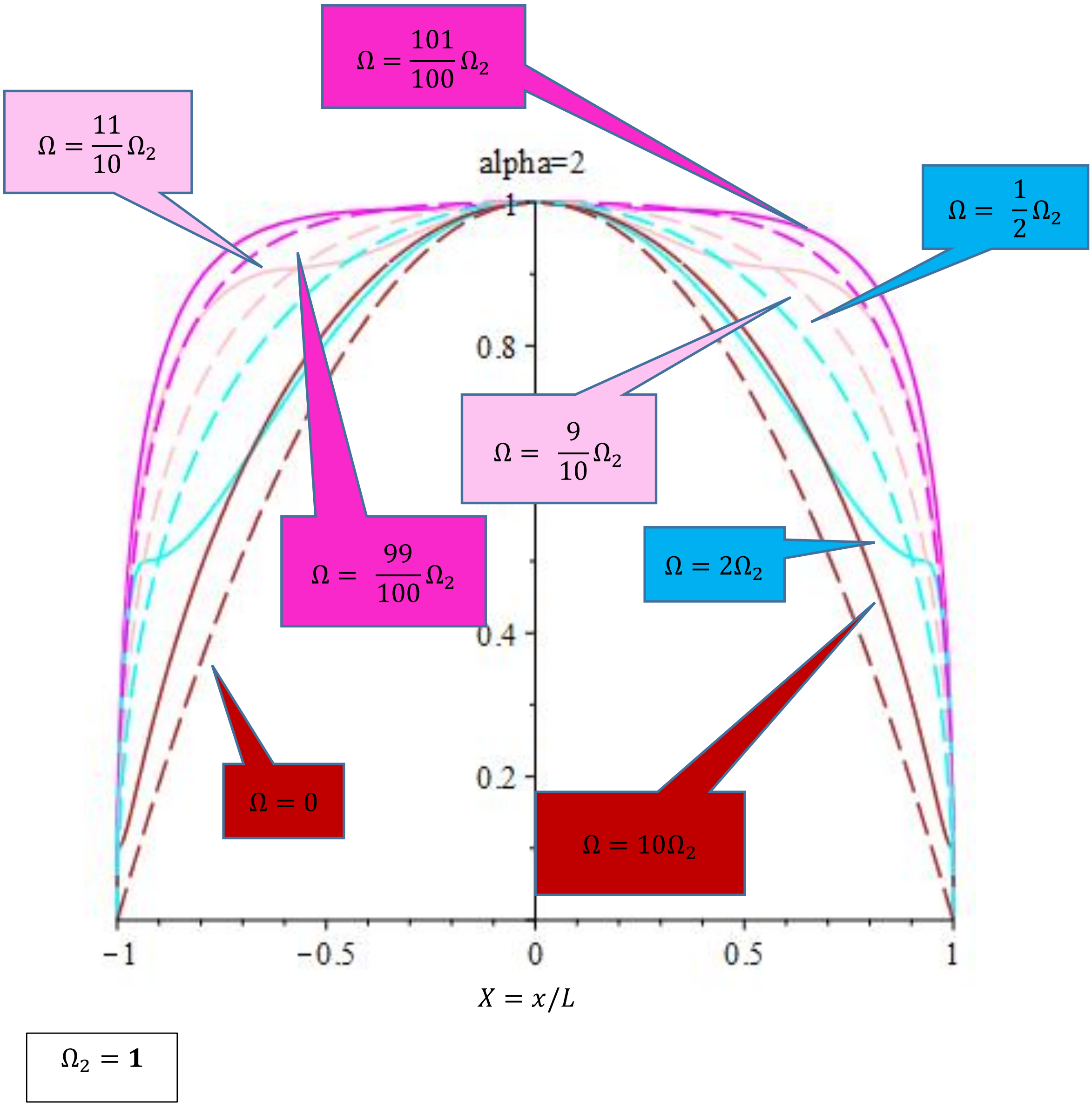

Figure 5 Areas of cross-sections of the optimal twisted rods for $\alpha = 2$ for all values of parameter Ω

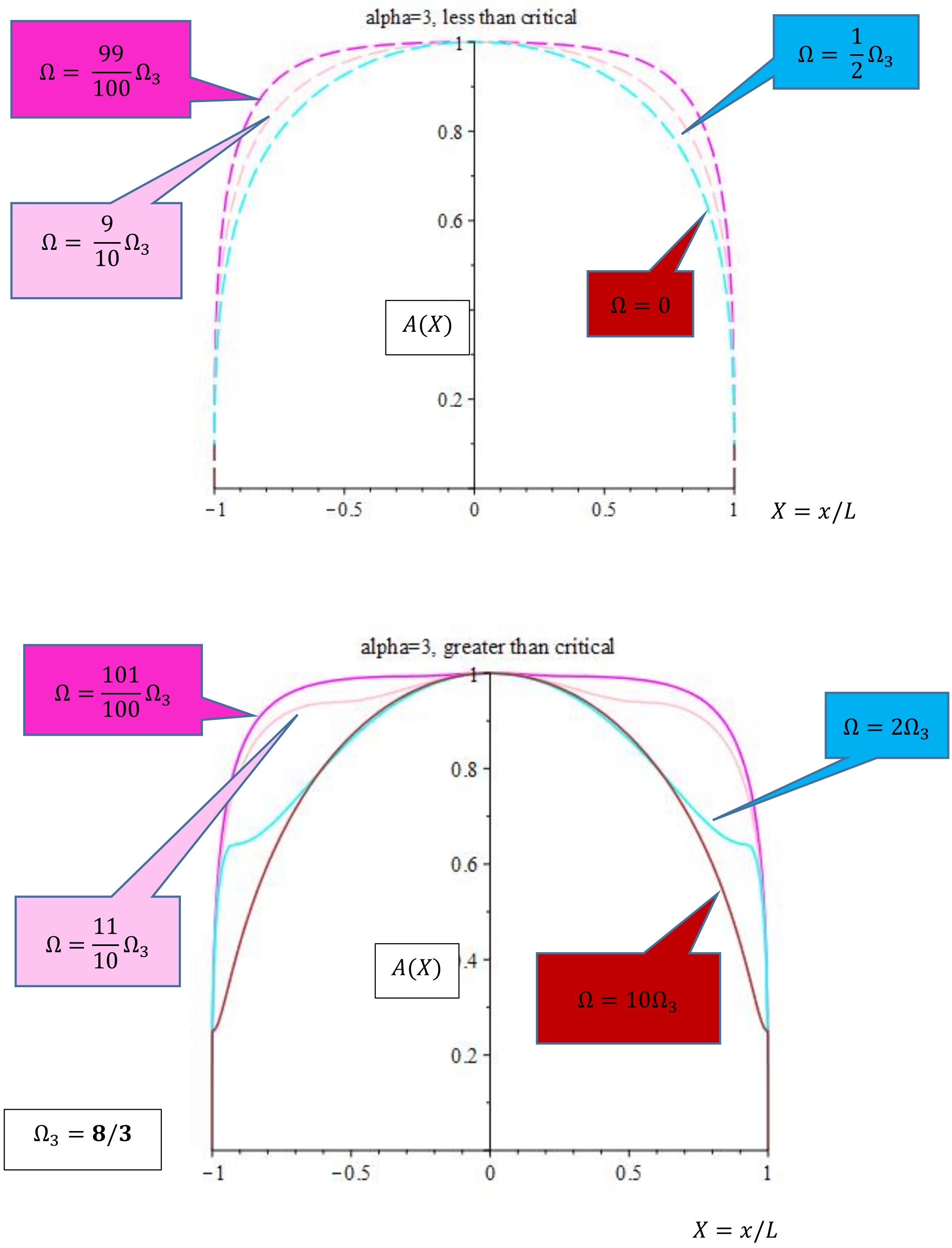

Figure 6 Areas of cross-sections of the optimal twisted rods for $\alpha = 2$ for all values of parameter Ω

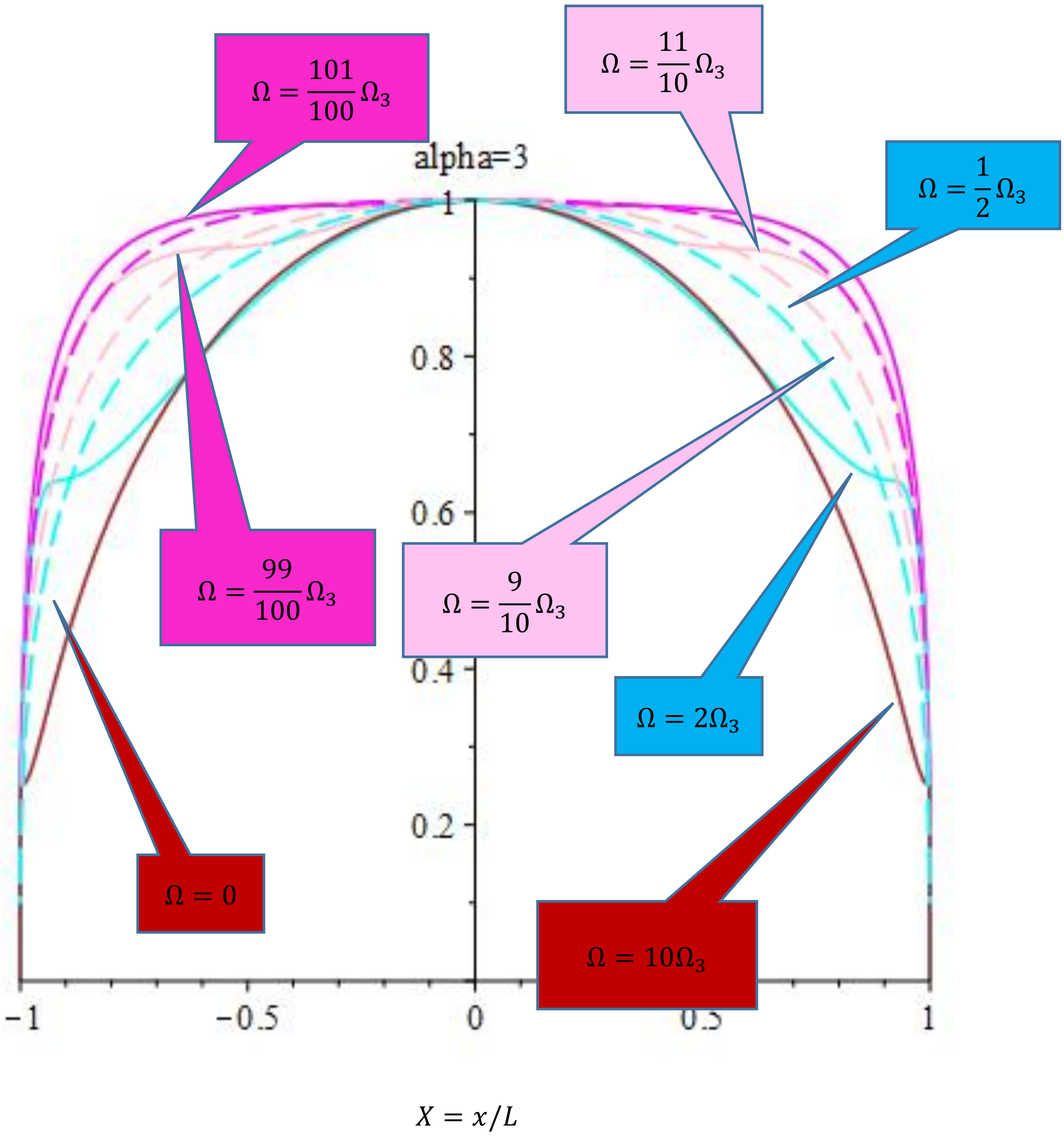

$\Omega_3 = \mathbf{8/3}$

Figure 7 Areas of cross-sections of the optimal twisted rods for $\alpha = 2$ for all values of parameter Ω

v_{ref}

for $L=1$

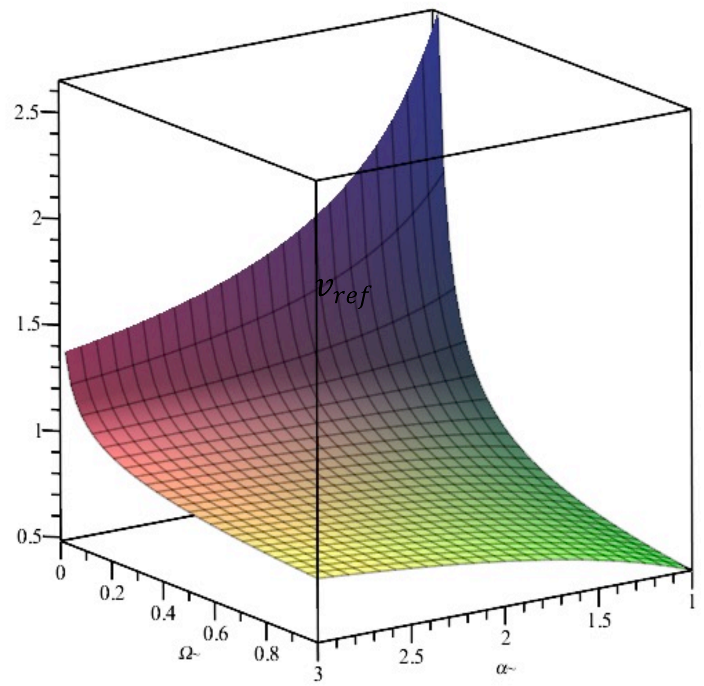

Figure 8 Volumes of the reference rods with the constant cross-sections for different α and Ω and $L=1$

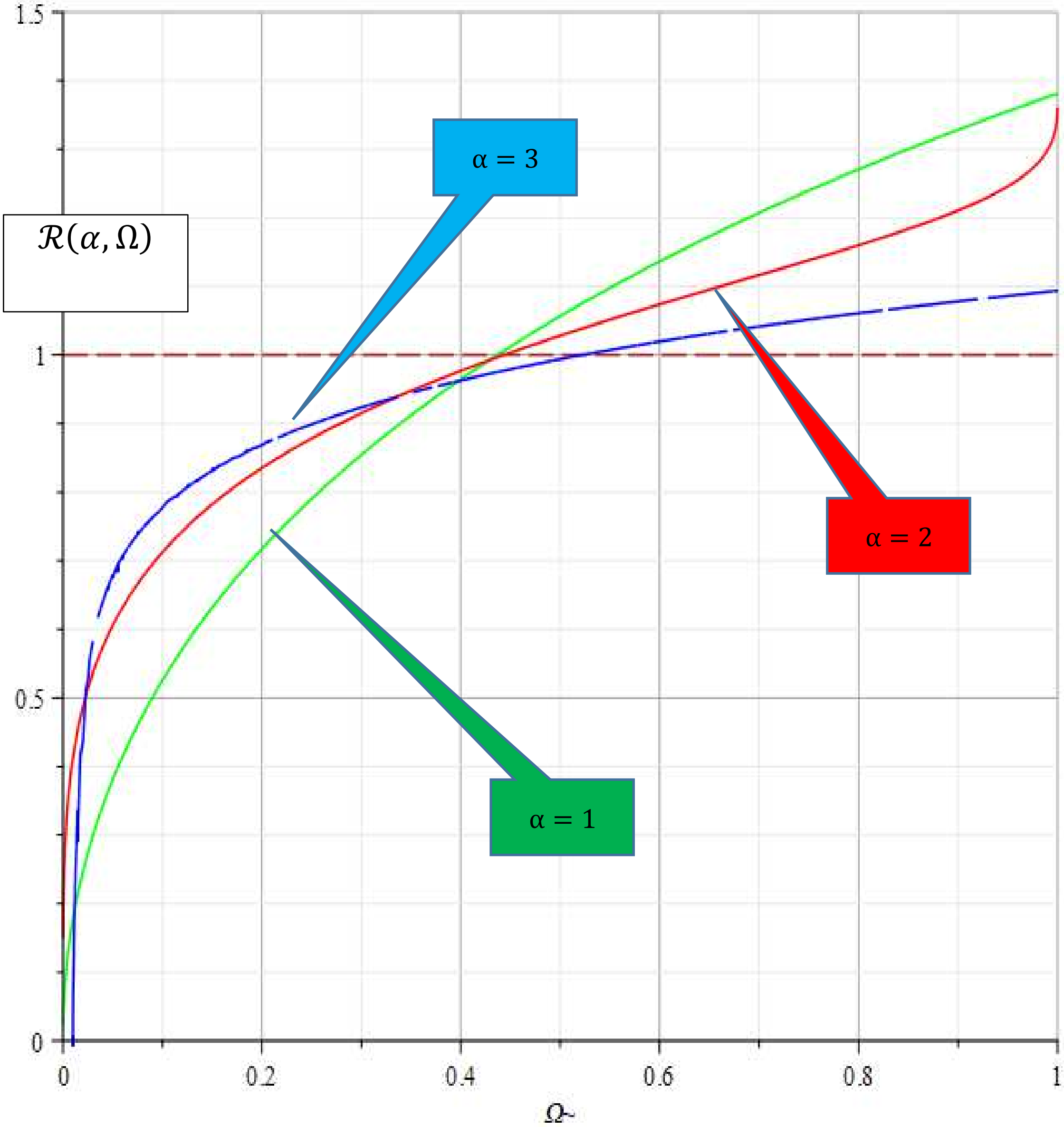

Figure 9 Relations $\mathcal{R}(\alpha,\Omega)$ of masses of optimal rods to the masses of the rods with the constant cross-sections for $\alpha = 1,2,3$

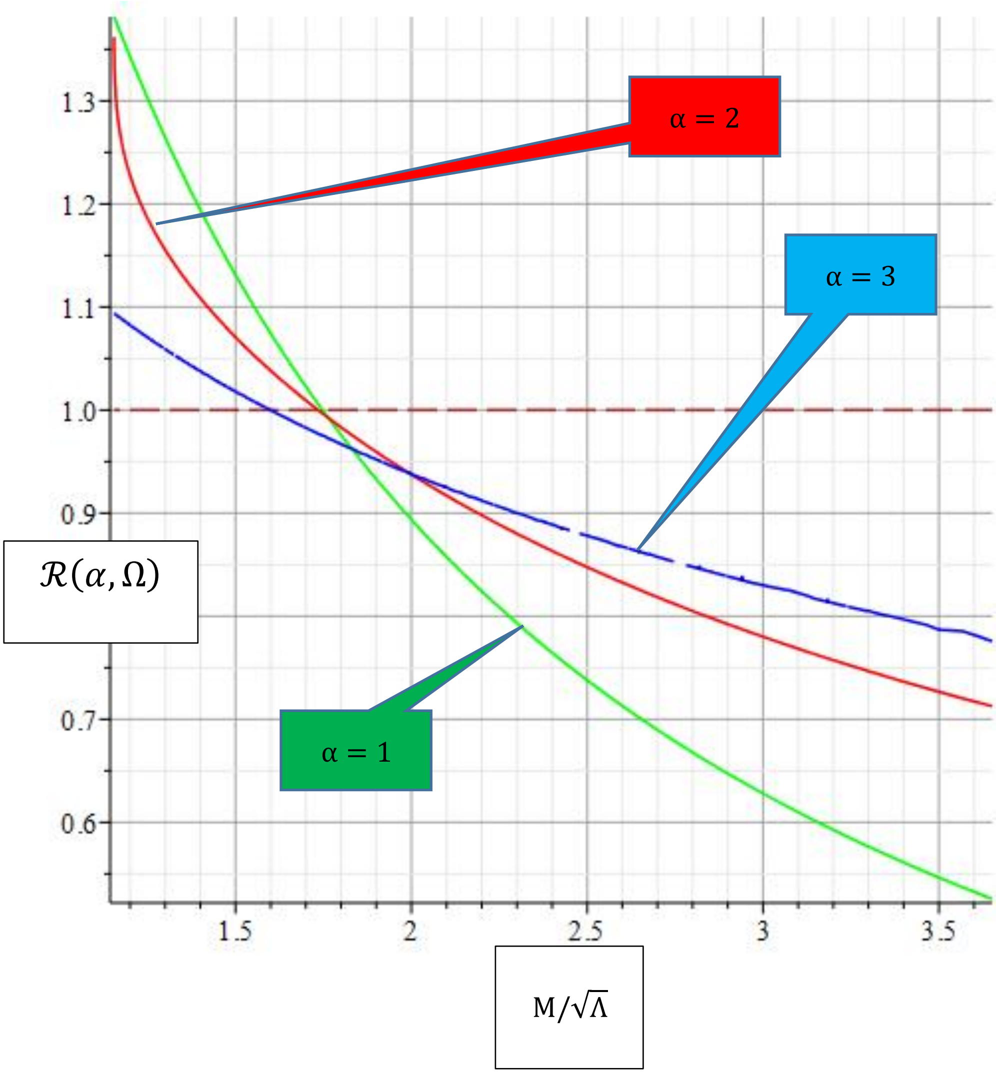

Figure 10 Relations $\mathcal{R}$ *of masses of optimal rods to the masses of the rods with the constant cross-sections as functions of* $\mathrm{M}/\sqrt{\Lambda}$ *and* $\alpha = 1,2,3$

Figures

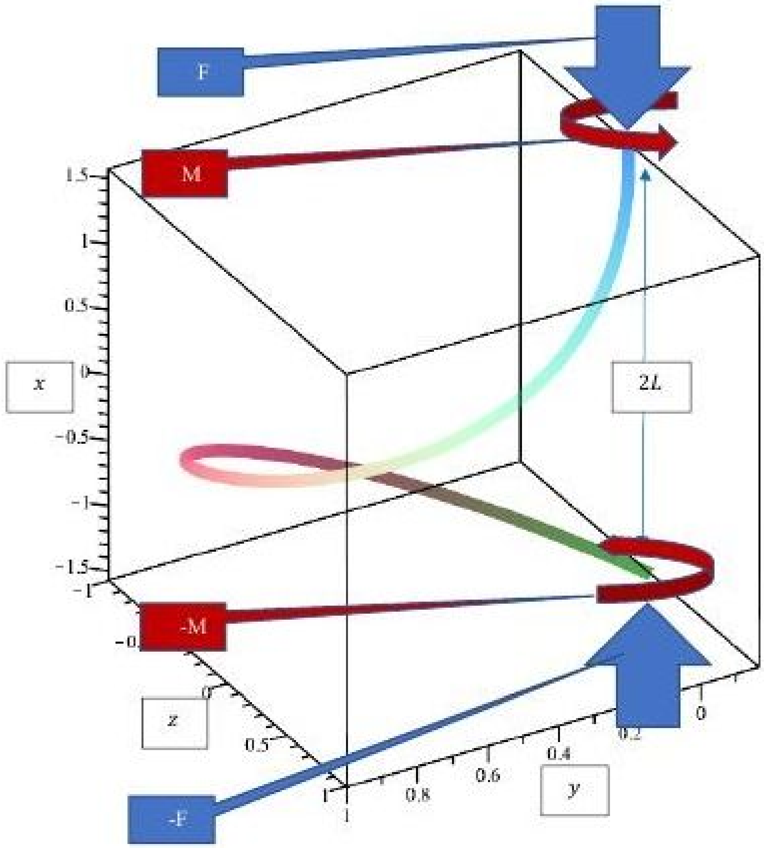

Figure 1 The buckling shape of the simultaneously twisted and compressed rod with the simply supported (hinged) ends.

Figure 1

The buckling shape of the simultaneously twisted and compressed rod with the simply supported (hinged) ends

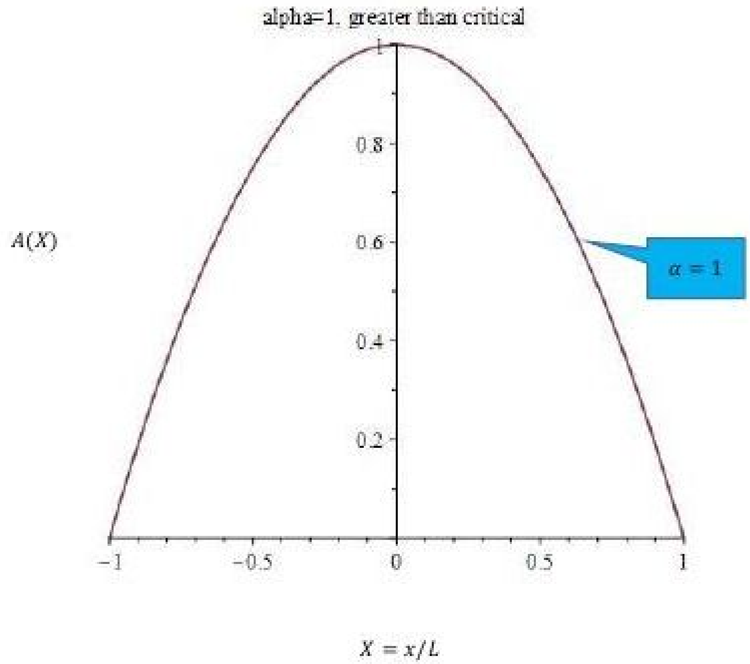

Figure 2 Areas of cross-sections of the optimal twisted rods for $\alpha = 1$ for all values of parameter Ω

Figure 2

Areas of cross-sections of the optimal compressed/twisted rods for α=1 for all values of parameter Ω

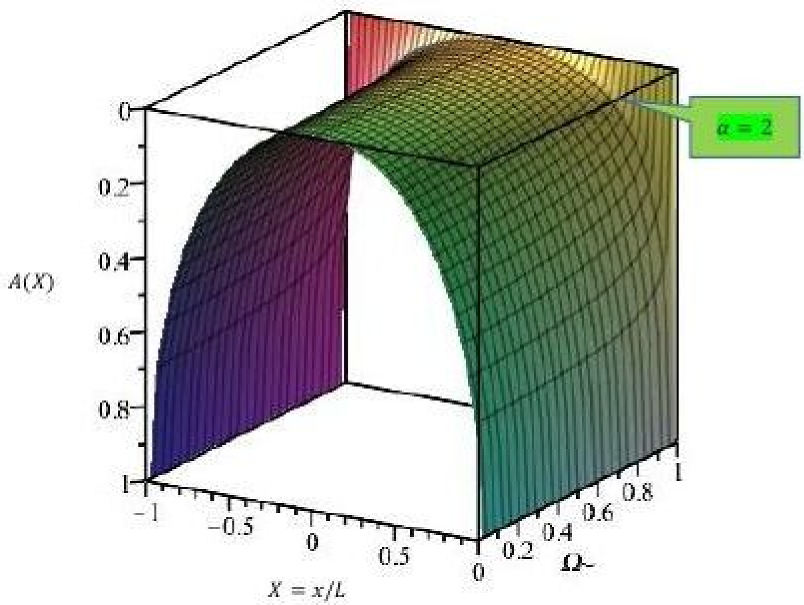

Figure 3 Areas of cross-sections of the optimal twisted rods for $\alpha = 2$ for all values of parameter Ω

Figure 3

Areas of cross-sections of the optimal compressed/twisted rods for α=2 for all values of parameter Ω

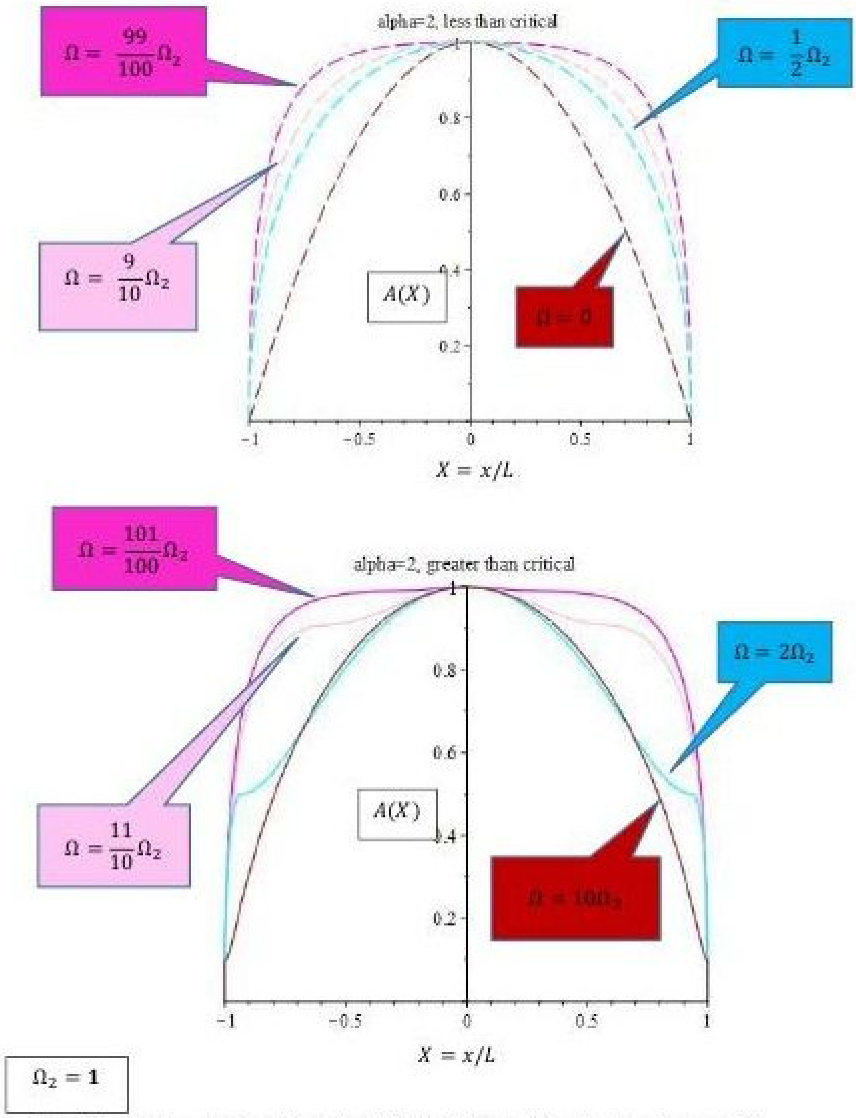

Figure 4 Areas of cross-sections of the optimal twisted rods for $\alpha = 2$ for all values of parameter Ω

Figure 4

Areas of cross-sections of the optimal compressed/twisted rods for α=2 for all values of parameter Ω

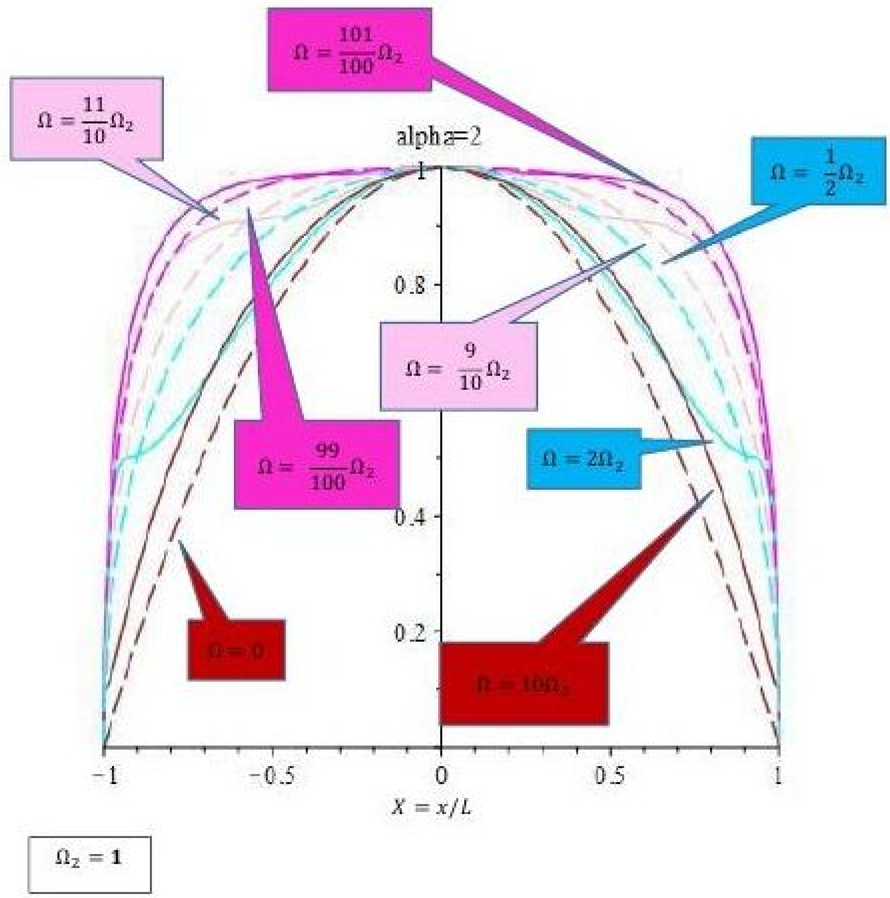

Figure 5 Areas of cross-sections of the optimal twisted rods for $\alpha = 2$ for all values of parameter Ω

Figure 5

Areas of cross-sections of the optimal compressed/twisted rods for α=2 for all values of parameter Ω

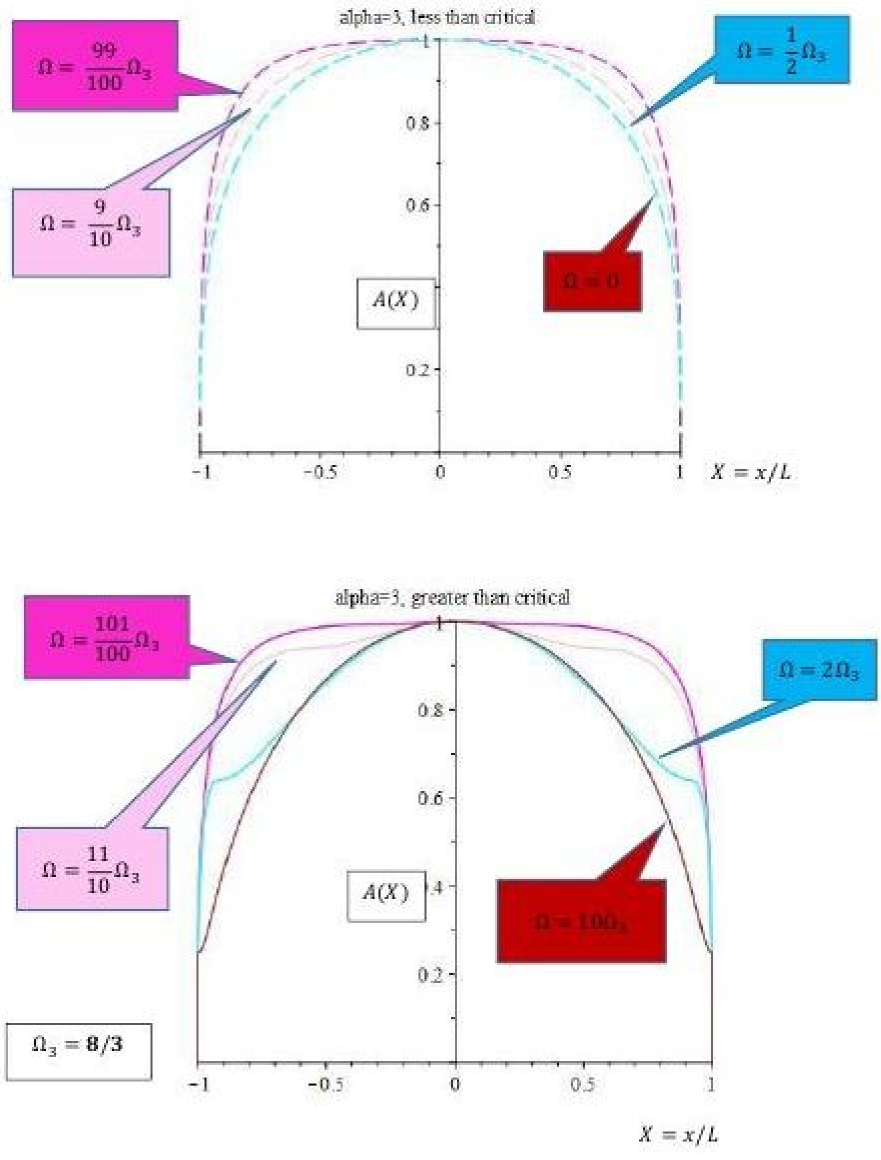

Figure 6 Areas of cross-sections of the optimal twisted rods for $\alpha = 2$ for all values of parameter Ω

Figure 6

Areas of cross-sections of the optimal twisted rods for α=2 for all values of parameter Ω

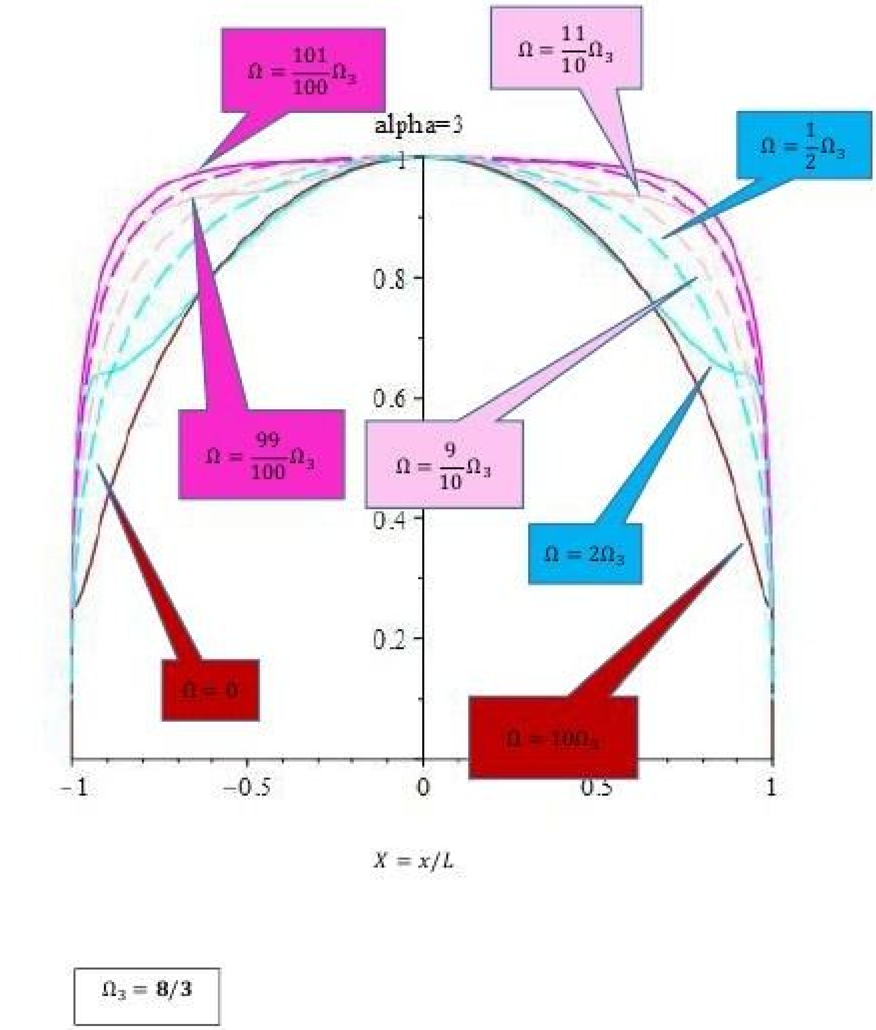

Figure 7 Areas of cross-sections of the optimal twisted rods for $\alpha = 2$ for all values of parameter Ω

Figure 7

Areas of cross-sections of the optimal twisted rods for α=2 for all values of parameter Ω

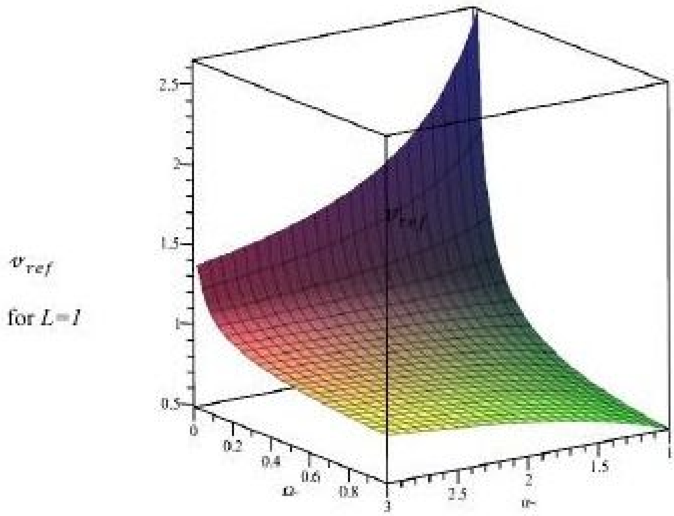

Figure 8 Volumes of the reference rods with the constant cross-sections for different α and Ω and L=1

Figure 8

Volumes of the reference rods with the constant cross-sections for different α and Ω and L=1

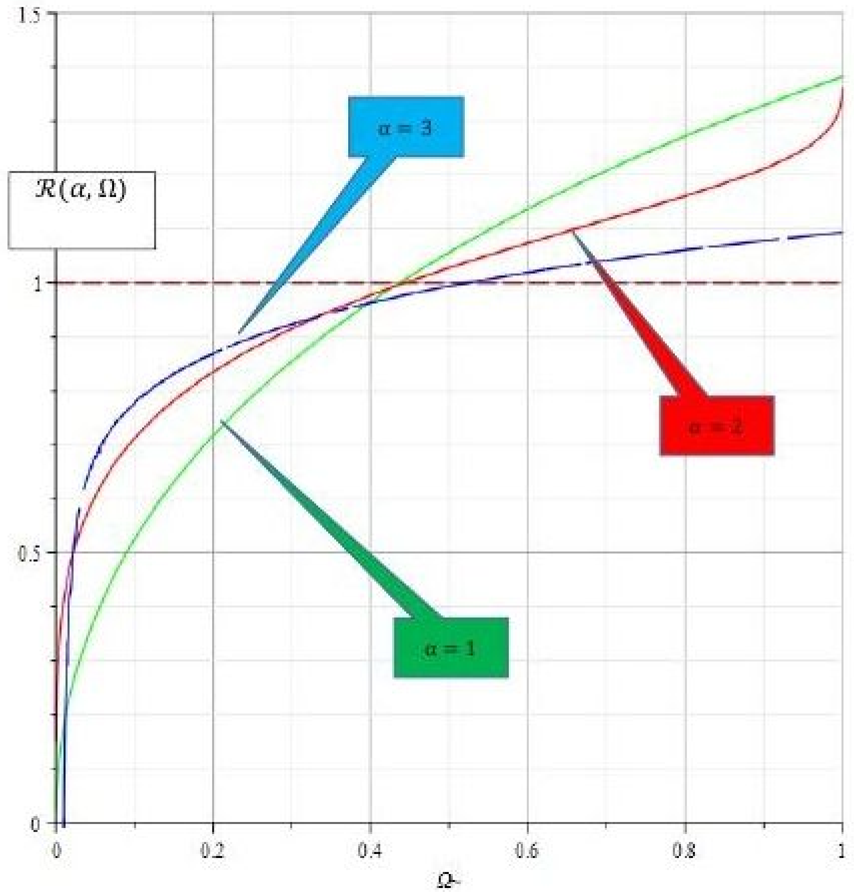

Figure 9 Relations $\mathcal{R}(\alpha,\Omega)$ of masses of optimal rods to the masses of the rods with the constant cross-sections for $\alpha = 1,2,3$

Figure 9

Relations R(α,Ω) of masses of optimal rods to the masses of the rods with the constant cross-sections for α=1,2,3

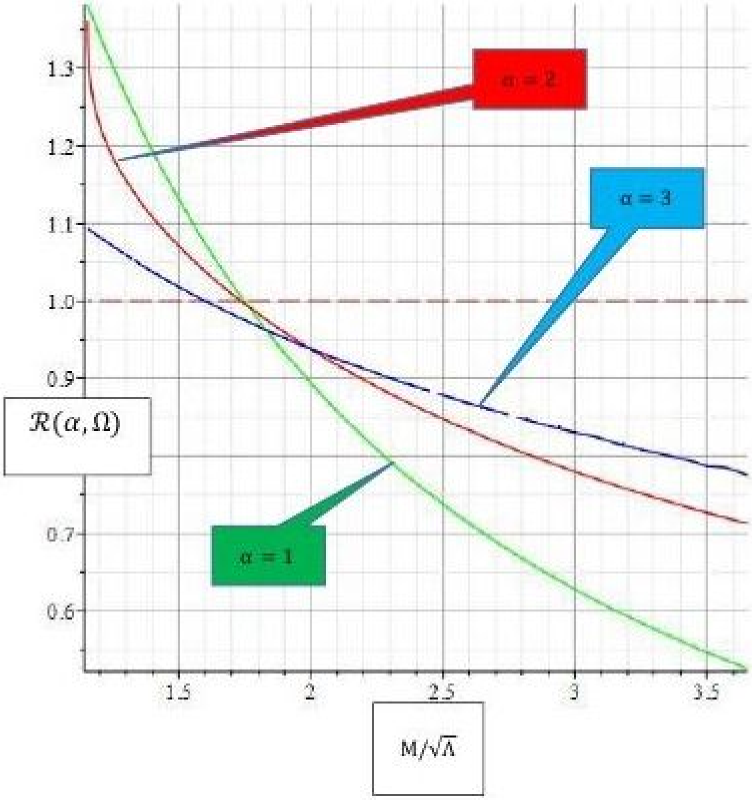

Figure 10 Relations $\mathcal{R}$ of masses of optimal rods to the masses of the rods with the constant cross-sections as functions of $\mathrm{M}/\sqrt{\Lambda}$ and $\alpha = 1.2.3$

Figure 10

Relations R of masses of optimal rods to the masses of the rods with the constant cross-sections as functions of M/√Λ and α=1,2,3